ORIGINAL ARTICLE

Role of diffusion weighted imaging and dynamic contrast enhanced magnetic resonance imaging in breast tumors

Magda Ali Hany El Bakry [a,1], **Amina Ahmed Sultan** [a,2],
Nahed Abd Elgaber El-Tokhy [a,3], **Tamer Fady Yossif** [b,4],
Carmen Ali Ahmed Ali [a,*]

[a] *Diagnostic Radiology, Faculty of Medicine, Mansura University, Egypt*
[b] *Surgical Oncology, Faculty of Medicine, Mansura University, Egypt*

Abstract *Purpose:* To evaluate the role of diffusion weighted imaging and dynamic contrast enhanced magnetic resonance imaging in characterization of breast tumors and comparing the results with the histological finding.

Patients and methods: From January 2011 to January 2015, 71 patients with 74 suspicious breast lesions had performed breast DCE-MRI combined with DWI and the results were compared with the histopathological examination which was used as the standard diagnostic method.

Results: The study included 71 patients with 74 suspicious breast lesions, there were 38 benign lesions ((51.35%) and 36 malignant lesions (48.65%)).

DCE-MRI proved to have a sensitivity of 91.7%, and a specificity of 84.2%. ADC cutoff value to differentiate between benign and malignant lesions was 1.32×10^3 mm^2/s ($P < 0.001$). The diffusion weighted MRI proved to have a sensitivity of 94.4%, and a specificity of 92.1%.

The combined MRI protocol of DCEMRI and DWI proved to increase the sensitivity and specificity of breast MRI.

* Corresponding author. Tel.: +20 1062092229.
E-mail addresses: drmagdaa@hotmail.com (M.A.H. El Bakry), dr_aminasultan@yahoo.com (A.A. Sultan), Nahedgaber28@yahoo.com (N.A.E. El-Tokhy), tamerfadysurg@gmail.com (T.F. Yossif), Carmenali042@gmail.com (C.A.A. Ali).
[1] Tel.: +20 1222449377.
[2] Tel.: +20 1111030880.
[3] Tel.: +20 1003915395.
[4] Tel.: +20 1223912791.

Conclusion: DWI had a higher sensitivity and specificity than DCE-MRI. The combined MRI protocol of DCEMRI and DWI proved to increase sensitivity and specificity of MRI in diagnosis and differential diagnosis of breast lesions.

1. Introduction

Breast cancer is the commonest female cancer. It is the 2nd leading cause of death among female after lung cancer (1). Improvements in diagnosis of breast cancer are largely responsible for increasing rate of survival among breast cancer women (2).

Techniques of Magnetic resonance imaging (MRI) such as dynamic contrast-enhanced MRI (DCE MRI) and diffusion-weighted (DW) techniques are among those of interest, as they allow noninvasive digital biomarker measurements of tissue properties that are highly valuable for assessment of tumor progression (3).

Dynamic contrast-enhanced MRI (DCE MRI) sensitivity in diagnosis of breast cancer is relatively high ranging from 88% to 100% for invasive breast malignancies (4,5). However the reported specificity of DCE MR imaging has been largely variable, ranging from 37% to 97% (6).

DCE MRI specificity is variable depending on lesion criteria that used in differentiation between benign and malignant breast tumors (7).

The commonly used lesion criteria used for characterization of breast lesions by DCE MRI are lesions morphology and enhancement kinetics (8,9).

According to BIRAD MRI lexicon, morphological evaluation of breast lesions is done by evaluating its shape, margins, and enhancement characteristics, enhancement distribution, and internal enhancement pattern. Kinetic evaluation is done by detecting the initial and post-initial enhancement of the breast lesion (10).

In order to increase breast MRI specificity, diffusion-weighted imaging (DWI) was designed (10).

Diffusion-weighted imaging (DWI) is a noninvasive technique which measures the free water protons random motion and evaluates the exchange (diffusion) of water molecules among compartments of breast tissues. Rate of diffusion is varying between pathologic and nonpathologic breast tissues (11).

The quantitative value of water molecules diffusion between tissue components is expressed by apparent diffusion coefficient (ADC) value. This value is proved to be different between benign and malignant breast lesions (11).

From 2002, a lot of studies (12–19) have revealed the usefulness of breast DWI in differentiation of benign from malignant lesions of the breast. These studies proved that the sensitivity of breast DWI was in the range of 80–96% and its specificity was in the range of 46–91%. Yabuuchi et al. (20) concluded 92% sensitivity and 86% specificity and also Partridge et al. (21) concluded that there is 10% improvement in the PPV when combining DWI with dynamic contrast-enhanced MRI (DCE-MRI) in the differentiation of breast masses (7,8).

2. Patients and methods

2.1. Patients

This prospective study was carried out in the period between January 2011 and January 2015 in diagnostic radiology department of Mansoura University Hospitals. The study comprised 71 women (age range, 28–75 years; mean age 46.6 years) with 74 suspicious breast lesions based on physical examination, mammography and ultra-sonography.

2.1.1. Inclusion criteria

1. Patient with suspicious breast lesion at mammography or breast ultrasound or with suspicious clinical findings.
2. Patients who are suspected to have local regional recurrence after resection of malignant breast lesion.
3. Patients who are suspected to have tumor residual following chemotherapy or radiotherapy sessions.

2.1.2. Exclusion criteria

1. Patients with history of breast biopsy within 1 month.
2. Patients without a detectable lesion on MRI corresponding to clinically or mammographically defined lesion.
3. Patients without histopathologic confirmation of the lesion.
4. Contraindication to perform MRI examination (cardiac pacemaker, or metallic aneurysm clips).

All the patients underwent full history taking, general and local examination. All patients underwent diffusion weighted MRI and dynamic contrast enhanced MRI examination and the results of breast MRI were compared with the histopathological results that were used as the standard diagnostic method.

2.2. MR imaging protocol

All patients were examined using a 1.5-T magnetic resonance machine. All patients were examined in the prone position using dedicated breast coil. MR Imaging was done within 7–14 days of menstrual cycle in premenopausal women. Examination included image acquisition followed by image post-processing.

2.3. Image acquisition

The conventional MRI protocol included Localizing sagittal view (scout view), axial nonfat saturated T1WI obtained by FSE with the following imaging parameters: TR 450 ms, TE

14 ms, slice thickness 3 mm, field of view (FOV) 300–360 mm and matrix was 307×512, and Short TI inversion recovery (STIR) with the following parameters: TR 7000–9000 ms, TE 70 ms and inversion time (TI) was 150 ms, slice thickness was 3–4 mm with inter slice gap 1 mm, field of view (FOV) 300–360 mm and the matrix was 307×512. Dynamic contrast enhanced MRI was made in the axial plane with fat suppression by applying fat saturated pulse. The sequence used was FLASH 3 D GRE-T1W1 with the following parameters: TR 4–8 ms, TE 2 ms, flip angle 20°–25°, slice thickness 2 mm with no inter-slice gap, field of view (FOV) 300–360 mm and the matrix was 307×512. Dynamic contrast enhanced MRI was performed after injection of a bolus of gadopentetate dimeglumine, in a dose of 0.1 mmol/kg using an automated injector at a rate of 3–5 ml/s through a 18–20 gauge intravenous cannula inserted in an antecubital vein. Contrast injection was followed by a bolus injection of saline (total of 20 ml at 3–5 ml/s). Dynamic study consists of one precontrast and 5 postcontrast series, each of them took about 1.16 min with a break between the precontrast and postcontrast study about 20 s.

Diffusion-weighted images were obtained before dynamic images using a diffusion-weighted echo-planar imaging (EPI) sequence with parallel imaging. Sensitizing diffusion gradients in three orthogonal directions with b values of 0, 500, and 1000 s/mm^2 were applied. The ADC maps were created automatically and the ADC values were calculated.

2.4. Image post-processing

Image postprocessing includes Image subtraction which was obtained by subtracting each of pre-contrast images from each post-contrast series images, Creation of time to signal intensity curves for suspicious enhancing lesions, and maximum intensity projection (MIP) views obtained through each orthogonal plane, producing sagittal, coronal and axial projections.

2.5. MRI interpretation

STIR images were first examined to detect the presence or absence of any lesion or cysts. In dynamic contrast enhanced MRI the type of lesion enhancement (mass or non-mass-like enhancement) was determined and morphologic features were analyzed. For mass enhancement lesions, the shape, margins, signal intensity on STIR and T1 weighted images were assessed as well as enhancement characteristics of the lesion. For non-mass lesions, the distribution of enhancement, internal enhancement pattern, and symmetry were evaluated.

Evaluation of enhancement kinetics of the lesion was done by detecting the peak percentage of signal intensity increase at the early postcontrast phase, (wash-in rate) and the shape of the curve after the early phase enhancement (washout kinetics). A wash-in rate of $> 80\%$ was defined as strong enhancement, between 50% and 80% as intermediate enhancement, and $< 50\%$ as slow enhancement. Types of curves were defined according to delayed-phase enhancement as persistent type I curve (continuing steady signal intensity increase throughout the dynamic course), plateau type II curve (signal intensity does not change in the delayed phase), and washout type III curve (more than 10% loss of the signal intensity over the time).

MRI BI-RADS classification was done for each lesion based on the combination of morphologic and kinetic criteria.

DWI was then evaluated regarding the signal intensity and the mean ADC of each lesion was measured by placing the ROI manually within the solid portion of the lesion.

2.6. Statistical analysis

Data were tabulated, coded and then analyzed using the computer program SPSS (Statistical package for social science) version 17.0.

2.7. Descriptive data

Descriptive statistics were calculated in the form of

1. Mean $\pm$ Standard deviation (SD).
2. Median and range (Minimum – maximum).
3. Frequency (Number-percent).

2.8. Analytical statistics

In the statistical comparison between the different groups, the significance of difference was tested using one of the following tests:

1. Student's t-test used to compare between mean of two groups of numerical (parametric) data.
2. Mann–Whitney U-test used to compare between mean of two groups of numerical (non-parametric) data.
3. Inter-group comparison of categorical data was performed by using chi square test (X^2-value).

The sensitivity, specificity, positive predictive value, negative predictive value and accuracy were calculated for dynamic MRI and DWI. Also ADC was examined at different cutoff points using ROC curve analysis to determine the best cutoff point as well as the diagnostic power of each test.

A P value < 0.05 was considered statistically significant.

3. Results

All 71 patients compromised in this study underwent both DCE-MRI and DWI for their suspicious breast lesions and they had a histopathologic reference standard test for their index lesion. Histopathologic analysis revealed benign lesion in 38 patients (51.35%) and malignant lesion in 36 patients (48.65%).

The histopathologic types of 38 benign lesions were as follow (Table 1): 14 lesions (36.8%) were fibroadenomas (Figs. 3 and 4), 6 lesions (15.8%) were fibrocystic changes (FCC) (Fig. 5), 5 lesions (13.2%) were mastitis (3 acute infectious mastitis and 2 chronic granulomatous mastitis), 5 lesions (13.2%) were fat necrosis, 4 lesions (10.5%) were postoperative scar, and 4 lesions (10.5%) were postoperative seroma.

The histopathologic types of 36 malignant lesions were as follows (Table 2): 20 lesions (55.6%) were invasive duct carcinoma (Fig. 7), 6 lesions (16.7%) were invasive lobular carcinoma, 3 lesions (8.3%) were mucinous carcinoma (Fig. 6), 3

Table 1 Histopathological diagnoses of 38 benign breast lesions.

Histopathological type of benign breast lesions	No	%
Fibroadenoma	14	36.8
Fibro cystic change (disease)	6	15.8
Mastitis	5	13.2
Fat necrosis	5	13.2
Postoperative scar	4	10.5
Postoperative seroma	4	10.5
Total	38	

Table 2 Histopathological diagnoses of 36 malignant breast lesions.

Histopathological type of malignant breast lesions	No	%
Invasive duct carcinoma	20	55.6
Invasive lobular carcinoma	6	16.7
Mucinous carcinoma	3	8.3
Medullary carcinoma	3	8.3
DCI	3	8.3
Metastasis	1	2.8
Total	36	

Table 3 Shows the side and site of breast lesions in correlation with histopathological results.

			Groups		P
			Benign	Malignant	
Side	RT	No	21	20	0.98
		%	55.3%	55.6%	
	LT	No	17	16	
		%	44.7%	44.4%	
Site	Upper outer quadrant	No	15	20	0.7
		%	39.5%	55.6%	
	Upper inner quadrant	No	7	6	
		%	18.4%	16.7%	
	Lower outer quadrant	No	8	5	
		%	21.1%	13.9%	
	Lower inner quadrant	No	6	4	
		%	15.8%	11.1%	
	Retroareolar	No	2	1	
		%	5.3%	2.8%	

P: Probability.
Test used: chi-square test.

lesions (8.3%) were medullary carcinoma, 3 lesions (8.3%) were ductal carcinoma in situ (DCI) (Fig. 8), and 1 lesion (2.8%) was metastasis from squamous cell carcinoma of the right cheek.

According to the side of the lesions there were 21 benign lesions and 20 malignant lesions on the right breast and 17 benign lesions and 16 malignant lesions on left breast (Table 3).

According to the site of breast lesions, there were 35 lesions in the upper outer quadrant (15 were benign lesions and 20 were malignant lesions), 13 lesions in upper inner quadrant (7 were benign lesions and 6 were malignant lesions), 13 lesions

in lower outer quadrant (8 were benign lesions and 5 were malignant lesions), 10 lesions in lower inner quadrant (6 were benign lesions and 4 were malignant lesions), and 3 lesions in retroareolar region (2 were benign lesions and 1 was malignant lesion) (Table 3).

The average size of the benign lesions was 2.8 cm with range 1–7 cm and the average size of malignant lesions was 3 cm with range 1.5–6.5 cm (Table 4).

According to the shape of the lesions there were 7 rounded lesions all of them were benign 10 ovoid lesions: all of them were benign 14 lobulated lesions: 5 of them were benign and 9 were malignant; and 43 irregular lesion: 16 of them were benign and 27 were malignant (Table 5).

According to the margins of the lesions there were 22 smooth margin lesions: all of them were benign; 28 irregular margin lesions: 8 of them were benign and 20 were malignant; and 24 speculated margin lesion: 8 of them were benign and 16 were malignant (Table 5).

According to contrast enhancement pattern of the lesions homogenous enhancement was noted in 20 lesions: 14 lesions were benign and 6 lesions were malignant; heterogeneous enhancement was noted in 35 lesions: 8 lesions were benign and 27 lesions were malignant; rim enhancement was noted in 16 lesions: all of them were benign; and nonmass enhancement was noted in 3 lesions: all of them were malignant (Table 6).

According to the enhancement kinetics wash in rate was slow (< 50%) in 16 lesions: all of them were benign; intermediate wash in rate (50–80%) in 22 lesions: 20 lesion were

Table 4 Comparison between histopathological results as regards size of lesions.

		Benign	Malignant	P
Size (cm)	Median	2.8	3.0	0.47
	Range	1.0–7.0	1.5–6.5	

P: Probability.
Test used: Mann–Whitney U test.

Table 5 Shows the morphologic characteristics of breast lesions (as regards the shape and margin) in correlation with histopathological results.

			Benign	Malignant	P
Shape	Rounded	No	7	0	< 0.0001
		%	18.4%	0.0%	
	Ovoid	No	10	0	
		%	26.3%	0.0%	
	Lobulated	No	5	9	
		%	13.2%	25.0%	
	Irregular	No	16	27	
		%	42.1%	75.0%	
Margin	Smooth	No	22	0	< 0.0001
		%	57.9%	0.0%	
	Irregular	No	8	20	
		%	21.1%	55.6%	
	Speculated	No	8	16	
		%	21.1%	44.4%	

P: Probability.
Test used: chi-square test.

Table 6 Shows the enhancement pattern and enhancement kinetics (as regards wash in rate and shape of time/signal intensity curve) of breast lesions in correlation with histopathological results.

		Groups				P
		Benign		Malignant		
		No	%	No	%	
Enhancement pattern	Homogenous enhancement	14	36.8	6	16.7	< 0.0001
	Heterogeneous enhancement	8	21.1	27	75.0	
	Rim enhancement	16	42.1	0	0.0	
	Nonmass enhancement	0	0.0	3	8.3	
Wash in rate	Slow enhancement (< 50%)	16	42.1	0	0.0	< 0.0001
	Intermediate enhancement (50–80%)	20	52.6	2	5.6	
	Strong enhancement (> 80%)	2	5.3	34	94.4	
Shape of time/SI curve	Persistent type I	34	89.5	5	13.9	< 0.0001
	Plateau type II	3	7.9	9	25.0	
	Washout type III	1	2.6	22	61.1	

P: Probability.
Test used: chi-square test.

benign and 2 lesions were malignant; and strong wash in rate (> 80%) in 36 lesions: 2 lesions were benign and 34 lesions were malignant (Table 6).

According to shape of dynamic curve (time/signal intensity curve) type I (persistent curve) was noted in 39 lesions: 34 lesions were benign and 5 lesions were malignant; type II (plateau curve) noted in 12 lesions: 3 lesions were benign and 9 lesions were malignant; and type III (washout curve) noted in 23 lesions: 1 lesion was benign and 22 lesions were malignant (Table 6).

By comparing the DCE-MRI findings with histopathological findings there were 33 true-malignant lesions (BI-RADS 4 in 16 and BI-RADS 5 in 17), 32 true-benign lesions (BI-RADS 2 in 12 and BI-RADS 3 in 20), 6 misclassified benign lesions (misclassified as BI-RADS 4), and 3 misclassified malignant lesions (misclassified as BI-RADS 3).

DCE-MRI proved to have a sensitivity of 91.7%, a specificity of 84.2%, PPV of 84.6%, NPV of 91.4% and accuracy of 87.9% (Table 8).

In all 74 lesions, we could localize and measure the ADC value of each lesion. The median ADC of benign lesions was 2.05×10^{-3} mm^2/s (range 0.89–3.56×10^{-3}) and that of malignant lesions was 0.92×10^{-3} mm^2/s (range, 0.68–1.85×10^{-3}). ADC values were significantly lowered in malignant lesions compared with benign lesions ($p < 0.001$) (Fig. 1) (Table 7).

ROC curves of the ADC values are represented in Fig. 2. The cutoff value for ADC derived from the ROC analysis was 1.32×10^{-3} mm^2/s.

By comparing the diffusion weighted MRI findings with histopathological findings there were 34 true-malignant lesions, 35 true-benign lesions, 3 misclassified benign lesions, and 2 misclassified malignant lesions.

By comparing the combined results of both DCE-MRI and diffusion weighted MRI with histopathological findings there were 35 true-malignant lesions, 36 true-benign lesions, 2 misclassified benign lesions, and 1 misclassified malignant lesion.

The combined MRI protocol of DCEMRI and DWI proved to have a sensitivity of 97.2%, a specificity of 94.7%, PPV of 94.6%, NPV of 97.3% and accuracy of 95.9% (Table 8).
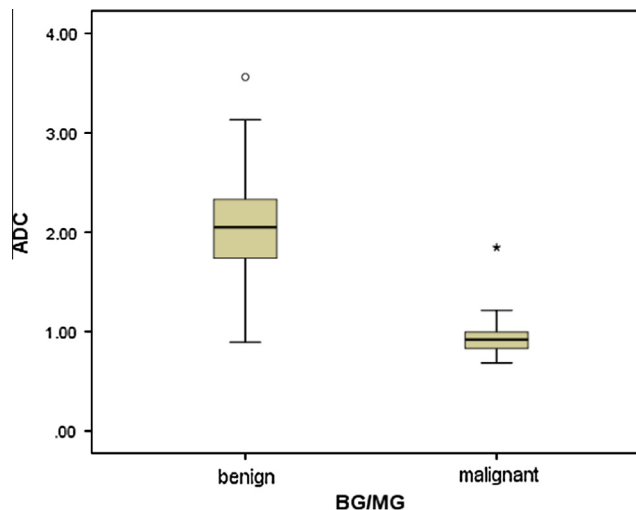

Fig. 1 Chart shows comparison between apparent diffusion coefficient (ADC) values of 38 benign and 36 malignant breast lesions. Median ADCs of benign and malignant breast lesions were 2.05 and 0.92×10^{-3} mm^2/s, respectively.

Table 7 Shows comparison between histopathological results as regards ADC.

		Groups		P
		Benign	Malignant	
ADC	Median	2.05	.92	< 0.0001
	Range	.89–3.56	.68–1.85	

P: Probability.
Test used: Mann–Whitney U test.

4. Discussion

This study included 71 patients with their age ranging from 28 to 75 years and mean age of 44.71 and 48.67 years for benign and malignant lesions respectively.
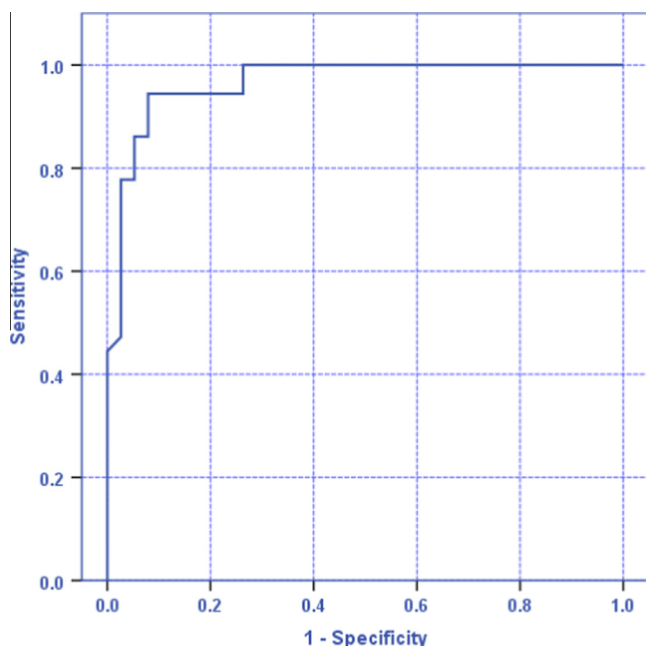
Fig. 2 Shows receiver operating characteristic (ROC) curve for apparent diffusion coefficient (ADC) values. Area under curve, which represents probability of lesion, will be classified accurately as benign or malignant according to ADC value, which is 0.97. Upper left point on curve is cutoff value of ADC which is 1.32×10^{-3} mm^2/s.

This is matched with the studies of Kriege et al., Warner et al., and Leach et al., as all had a mean age between 40 and 50 years (22–24).

The number of lesions included in this study was 74 lesions. Histopathologic analysis of these lesions revealed 38 benign lesions (51.35%) and 36 malignant lesions (48.65%).

In this study, the most common site for breast lesions was the upper outer quadrant 35 lesions (47.3%) followed by the upper inner and lower outer quadrants each has the same number of lesions (13 lesions in each) (17.6%). The 35 lesions in the upper outer quadrant included 15 benign and 20 malignant lesions, denoting that both benign and malignant lesions occur more frequently at this site.

This matches with Mahoney, and Darbre, who stated that the most common location of both benign and malignant lesions is in the upper outer quadrant. This may be due to the large amount of glandular tissue located in this region (25,26).

In this study, the two most common benign lesions were fibroadenoma and fibrocystic changes which represented 36.8% and 15.8% of benign lesions respectively while the two most common malignant lesions were invasive ductal carcinoma and invasive lobular carcinoma which represented 55.6% and 16.7% of malignant lesions respectively.

This matched with Li et al. who showed in their breast lesions survey that invasive ductal carcinoma accounts for 56%, fibroadenoma 20% and invasive lobular carcinoma 10% only (27).

In this study the most common shape of benign lesions was regular shape either ovoid or rounded shapes they represents 26.3% and 18.4% of benign lesions respectively while the shape of all malignant lesions was irregular or lobulated with high incidence for irregular shaped lesions 75% of all malignant lesions included in this study.

These results matched with Wedegärtner et al. and Tozaki et al. who showed that most benign lesions had ovoid or rounded shape while malignant lesions had irregular shape (28,29).

In this study the margins of benign lesions were variable with predominance of smooth margins (57.9%) of all benign lesions while the margins of malignant lesions were irregular or speculated and they represent 55.6% and 44.4% of all malignant lesions respectively.

These results matched with Mahoney et al. who reported that most of benign lesions showed smooth margins while malignant lesion showed irregular or speculated margins (30).

In this study according to enhancement pattern, homogenous enhancement was seen in 36.8% of benign lesions and 16.7% of malignant lesions, heterogeneous enhancement was seen in 21.1% of benign lesions and 75% of malignant lesions, rim enhancement was seen in 42.1% of benign lesions and none of malignant lesions and finally nonmass enhancement were seen in 8.3% of malignant lesions and none of benign lesions.

Morris, concluded that homogeneous enhancement is suggestive of a benign process; however, in small lesions, one must be careful as spatial resolution may limit evaluation. Also he concluded that the most frequent enhancement pattern among the malignant lesions was heterogeneous enhancement (96%) (31).

In this study wash in rate was slow ($< 50\%$) in 42.1% of benign lesions and none of malignant lesions, intermediate (50–80%) in 52.6% of benign lesions and 5.6% of malignant lesions, strong ($> 80\%$) in 5.3% of benign lesions and 94.4% of malignant lesions.

These results also matched with Kuhl et al. and Malich et al. who concluded that malignant lesions tend to exhibit strong and fast enhancement $> 80\%$ in the first 2 min after contrast injection (32,33).

Also these results matched with Kul et al. who showed that 95.7% of the malignant lesions revealed strong early enhancement (10).

In this study, according to shape of time/signal intensity curve, type I persistent curve was seen in 89.5% of benign lesions and 13.9% of malignant lesions, type II plateau curve was seen in 7.9% of benign lesions and 25% of malignant lesions, and type III washout curve was seen in 2.6% of benign lesions and 61.1% of malignant lesions.

These results matched with Kul et al. who showed that type I persistent curve was seen in 81.1% of benign lesions and 12.8% of malignant lesions, type II plateau curve was seen in 10.8% of benign lesions and 40.4% of malignant lesions, and type III washout curve was seen in 8.1% of benign lesions and 44.7% of malignant lesions (10).

In this study, the sensitivity and specificity of DCE-MRI examination were 91.7% and 84.2% respectively; this was based on the combination of morphologic and kinetic criteria.

These results disagree with Kul et al. who reported higher sensitivity (97.9%) and lower specificity (75.7%) than our study (10).

Our results also disagree with Hetta, and he proved that the sensitivity and specificity of DCE-MRI examination were 80% and 73.33% respectively (11).
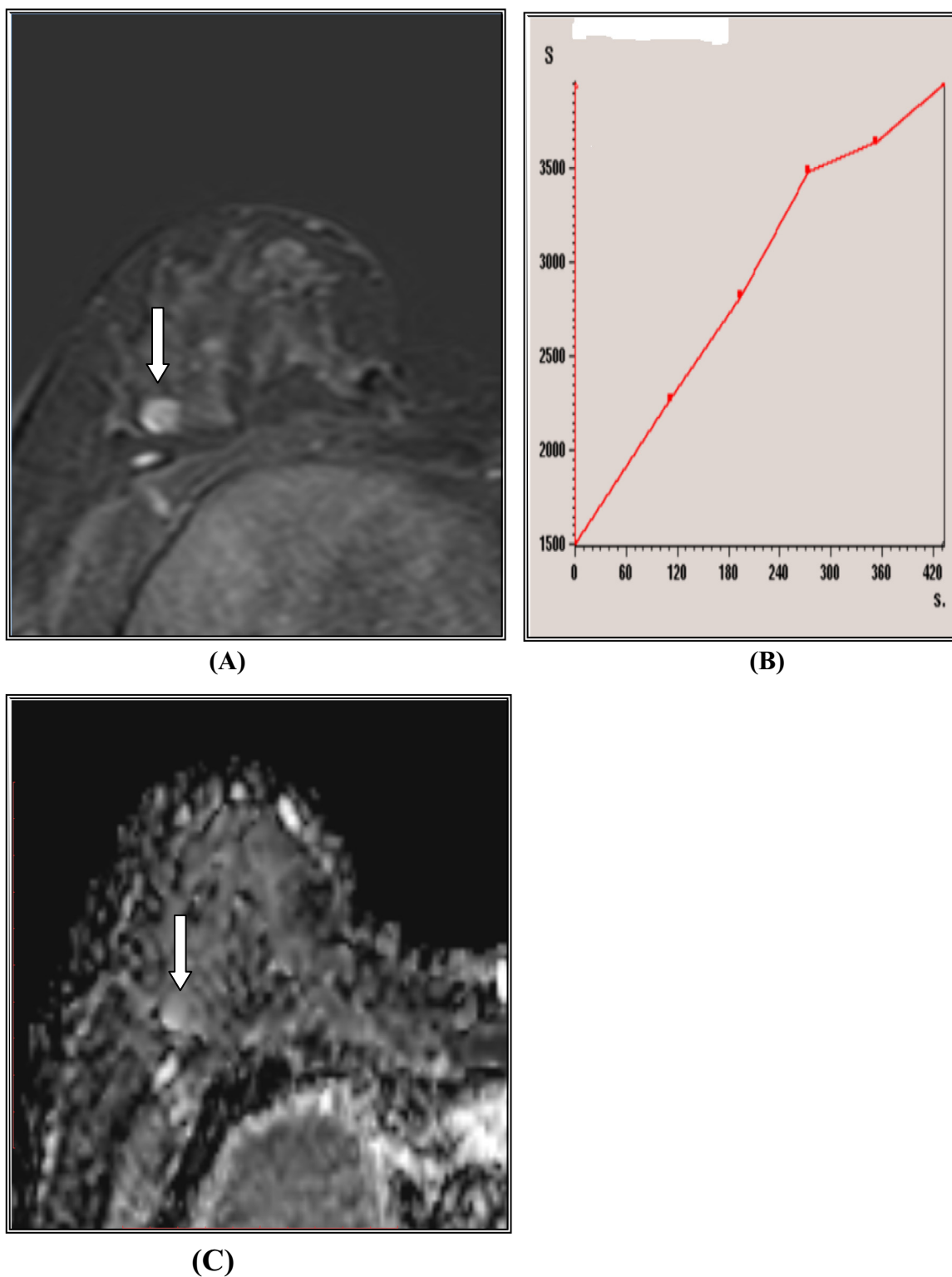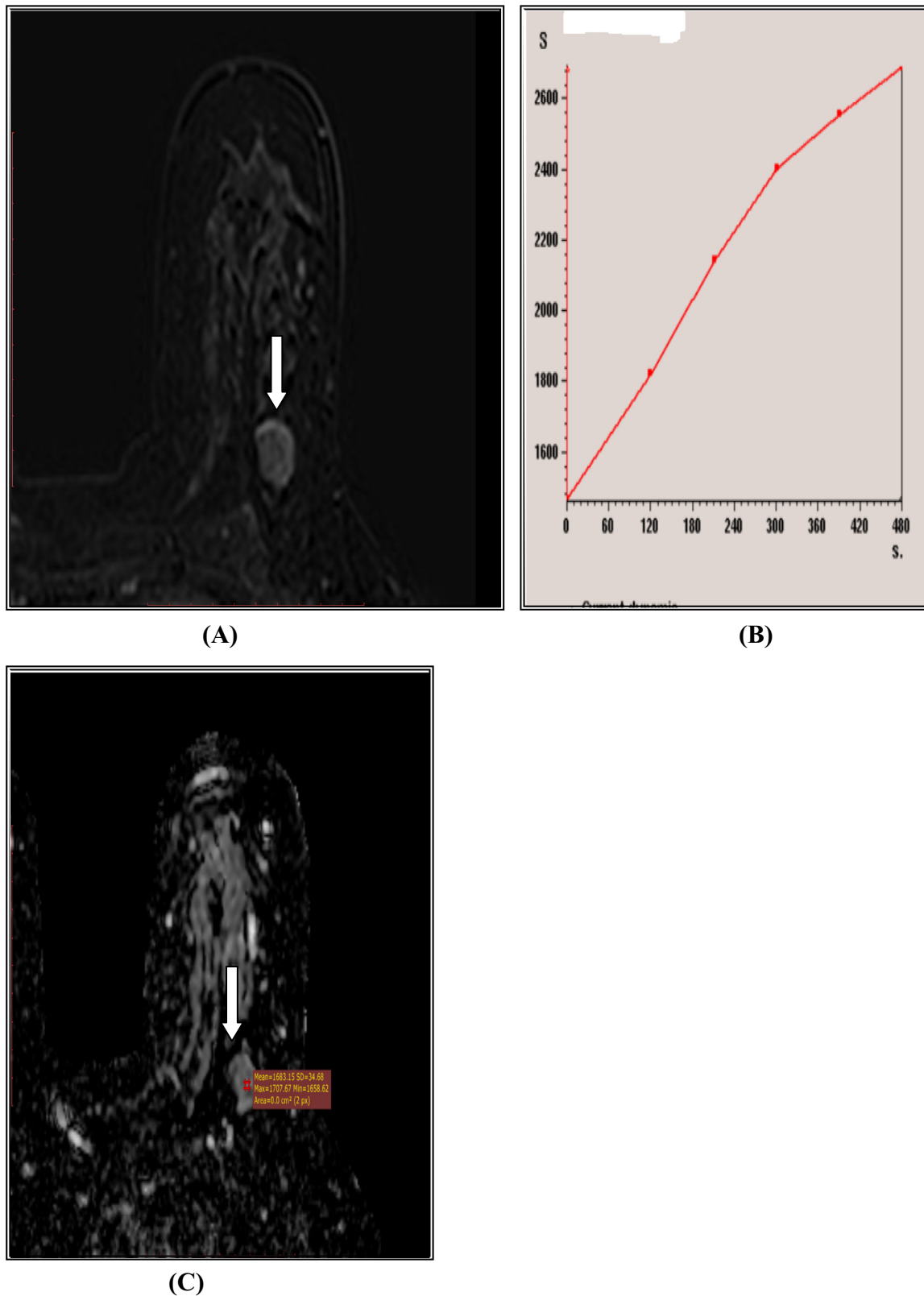
(A)

(B)

(C)

Fig. 3 Right breast fibroadenoma in 38-year-old woman. (A) dynamic contrast-enhanced subtracted image shows smooth marginated, round shaped mass with nonenhancing internal septation (arrow) in lower outer quadrant of right breast. (B) Time–signal intensity curve of mass shows type I persistent curve. (C) Apparent diffusion coefficient (ADC) map reveals increased diffusion (ADC $= 2.16 \times 10^{-3}$ mm^2/s) within mass. Mass was correctly classified as benign (BIRAD 3) according to combined imaging protocol.

(A)


(B)

(C)

Fig. 4   Left breast fibroadenoma in 50-year-old woman. (A) dynamic contrast-enhanced subtracted image shows well-marginated, ovoid-shaped mass with nonenhancing internal septation (arrow) in lower outer quadrant of left breast. (B) Time–signal intensity curve of mass shows type I persistent curve. (C) Apparent diffusion coefficient (ADC) map reveals increased diffusion (ADC $= 1.6 \times 10^{-3}$ mm^2/s) within mass. Mass was correctly classified as benign (BIRAD 3) according to combined imaging protocol.
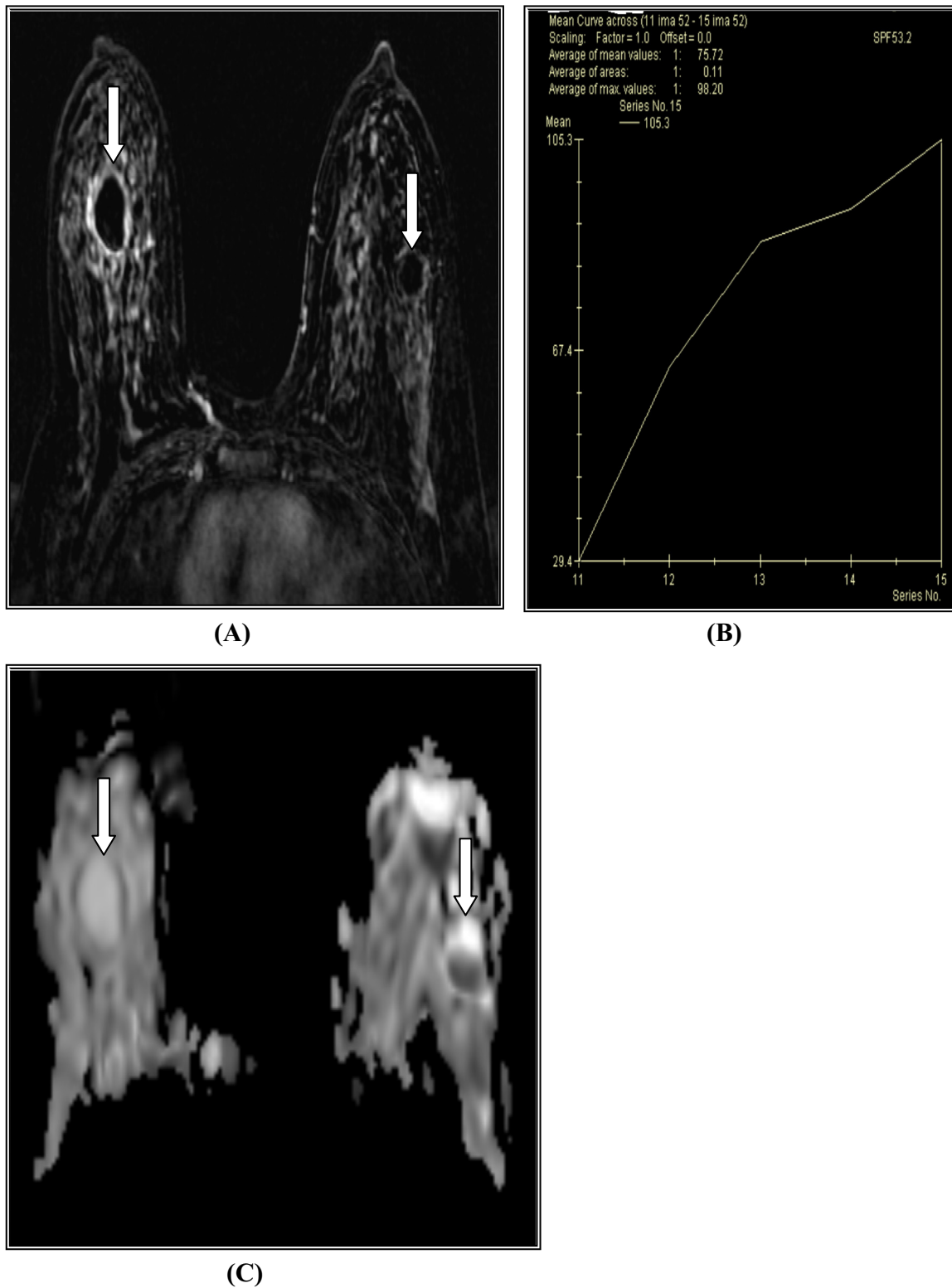
Fig. 5 Bilateral fibrocystic changes (FCC) in 48-year-old woman. (A) dynamic contrast-enhanced subtracted image shows bilateral well-marginated, ovoid-shaped cystic lesions with rim enhancement (arrows). (B) Time–signal intensity curve of the enhancing rim of the right sided lesion shows type I persistent curve. (C) Apparent diffusion coefficient (ADC) map reveals increased diffusion (ADC = $2.7–3.7 \times 10^{-3}$ mm^2/s) within right and left cysts respectively. Cysts were correctly classified as benign (BIRAD 2) according to combined imaging protocol.
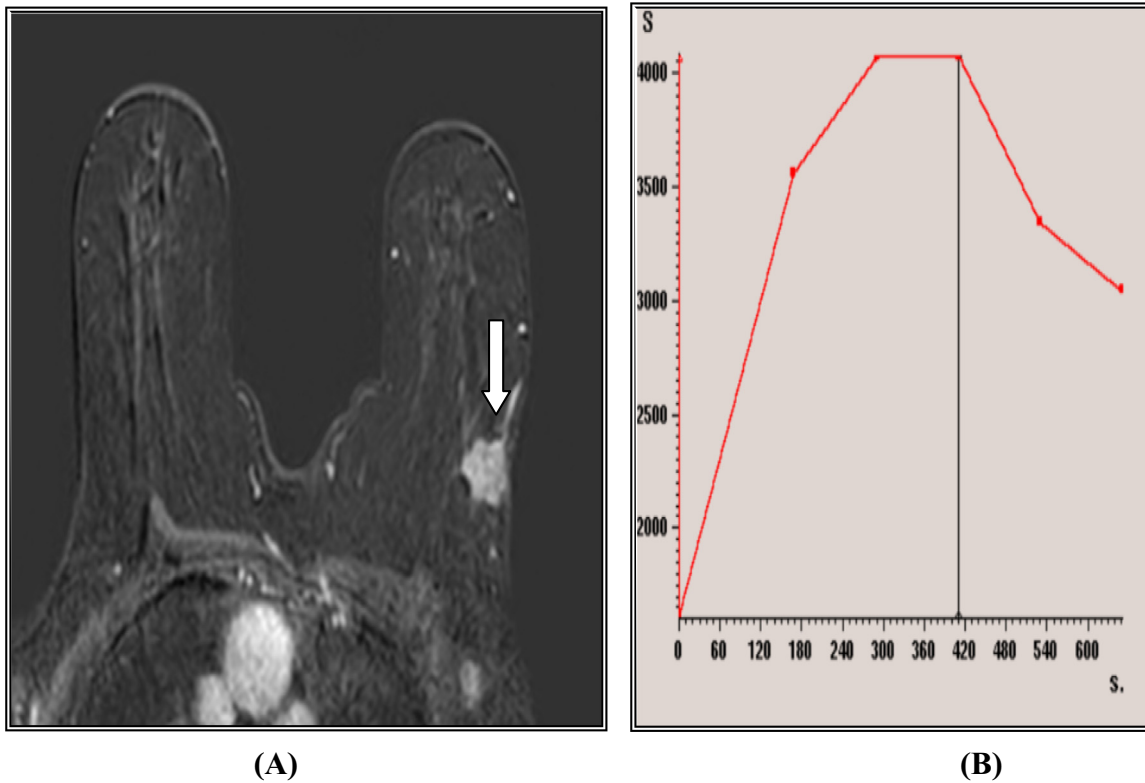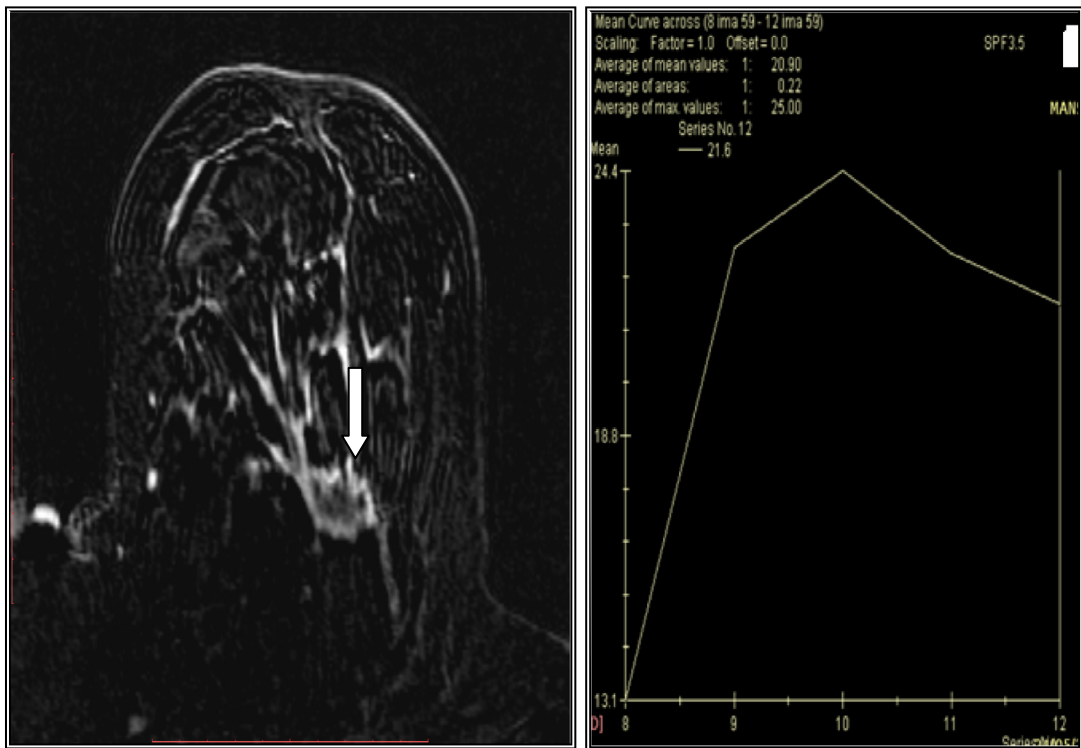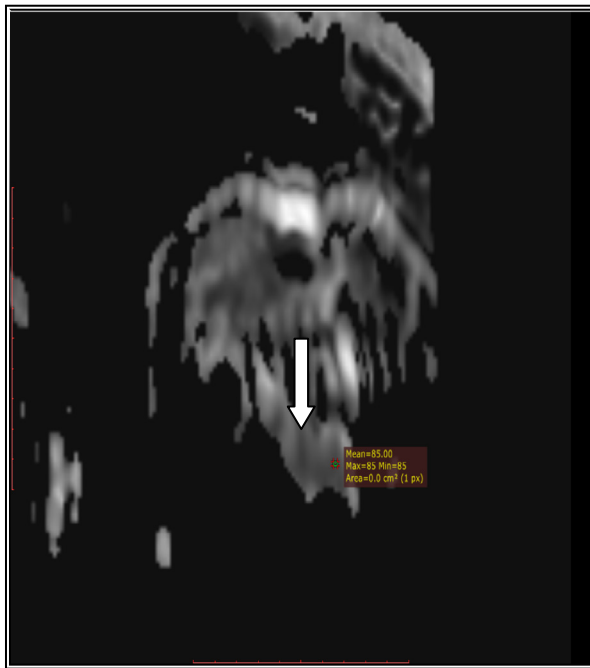
(A)

(B)

(C)

Fig. 6   Left breast grade II invasive lobular carcinoma in 70-year-old woman. (A) dynamic contrast-enhanced subtracted image shows irregular mass with speculated margins seen at the upper outer quadrant of left breast. (B) Time–signal intensity curve of mass shows type III washout curve. (C) Apparent diffusion coefficient (ADC) map reveals restricted diffusion (ADC $= 0.88 \times 10^{-3}$ mm^2/s) within mass. Mass was correctly classified as malignant (BIRAD 4b) according to combined imaging protocol.

(A)

(B)

(C)

Fig. 7   Left breast grade II invasive duct carcinoma in 48-year-old woman. (A) dynamic contrast-enhanced subtracted image shows irregular mass with speculated margins seen at the lower outer quadrant of left breast. (B) Time–signal intensity curve of mass shows type III washout curve. (C) Apparent diffusion coefficient (ADC) map reveals restricted diffusion (ADC $= 0.85 \times 10^{-3}$ mm^2/s) within mass. Mass was correctly classified as malignant (BIRAD 4b) according to combined imaging protocol.
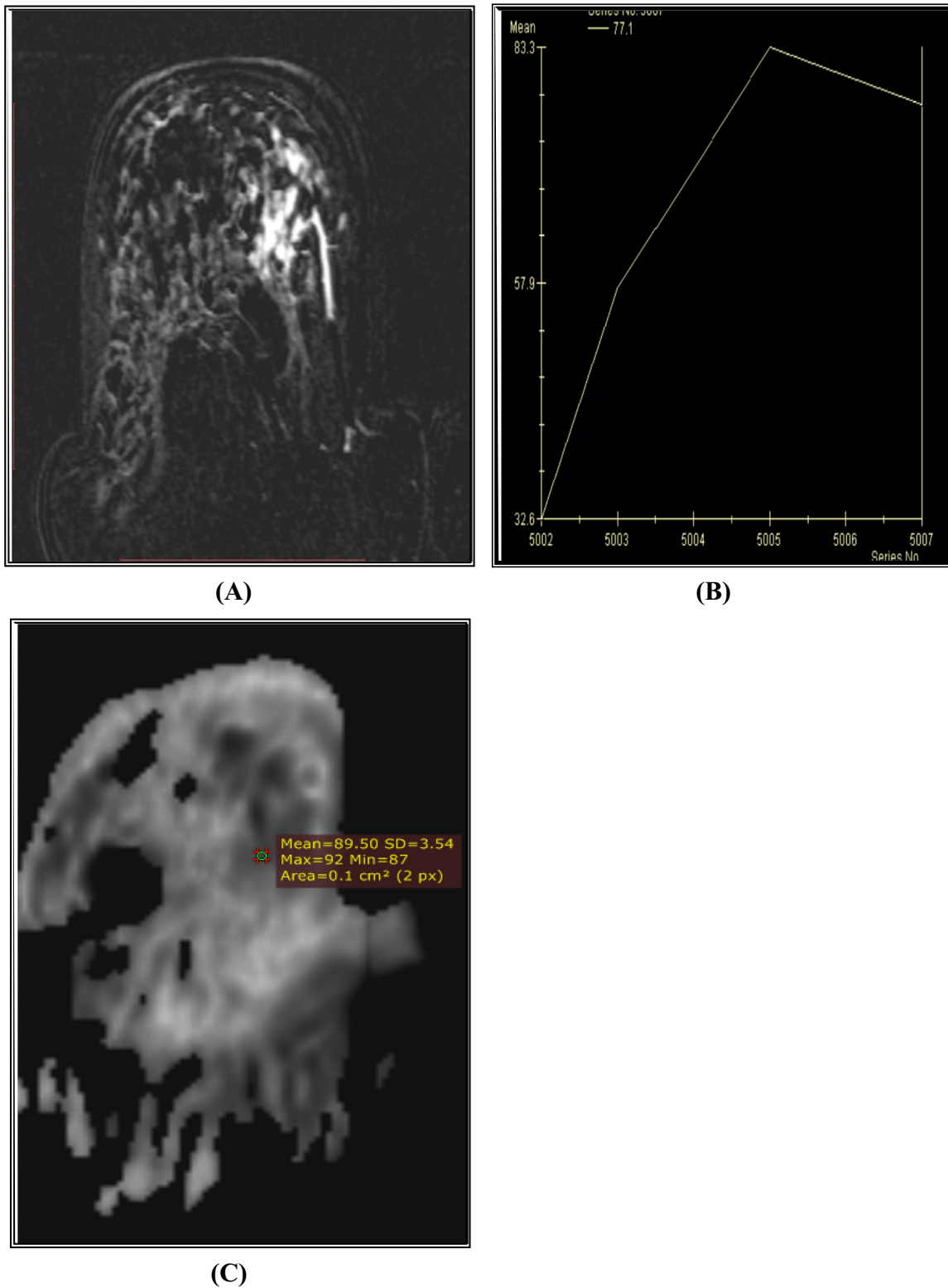
(A)

(B)

(C)

Fig. 8 Right breast grade II invasive duct carcinoma in 60-year-old woman. (A) Dynamic contrast-enhanced subtracted image shows irregular area of clumped non-mass-like enhancement on the lower inner quadrant of right breast. (B) Time–signal intensity curve of mass shows type III washout curve. (C) Apparent diffusion coefficient (ADC) map reveals restricted diffusion (ADC $= 0.89 \times 10^{-3}$ mm^2/s) within mass. Mass was correctly classified as malignant (BIRAD 4b) according to combined imaging protocol.

Table 8 Sensitivity and specificity of dynamic contrast-enhanced MRI (DCE-MRI), diffusion-weighted imaging (DWI), and combined MRI in 36 malignant and 38 benign breast lesions.

Results	DCE-MRI	DWI	Combined
Sensitivity (%)	91.7	94.4	97.2
Specificity (%)	84.2	92.1	94.7
PPV (%)	84.6	91.9	94.6
NPV (%)	91.4	94.6	97.3
Accuracy	87.9	93.2	95.9

In an attempt to increase the diagnostic efficacy of breast MRI, we evaluated the additional role of DWI.

In this study according to the lesion signal in diffusion weighted image, free diffusion showed 92.1% of benign lesions and 5.6% of malignant lesions, while restricted diffusion showed 7.9% of benign lesions and 94.4% of malignant lesions.

Kul et al., revealed the effectiveness of DWI for differentiating malignant from benign breast tumors. Consistent with this study, malignant lesions revealed significantly lower ADC values than benign lesions (10).

In this study the median ADC value of benign lesions was 2.05×10^{-3} mm^2/s (range 0.89–3.56 $\times 10^{-3}$ mm^2/s), and median ADC value of malignant lesions was 0.92×10^{-3} mm^2/s (range 0.68–1.85$^3 \times 10^{-3}$ mm^2/s).

These results disagree with Kul et al. who reported that the median ADC values of malignant and benign lesions were 0.75 and 1.26×10^{-3} mm^2/s, respectively (10).

This study showed that the best ADC cutoff value to differentiate between benign and malignant lesions was 1.32×10^{-3} mm^2/s. Malignant lesions exhibited lower mean ADC values compared with those of benign lesions.

These results match with Yabuuchi et al. who demonstrated an ADC value less than 1.3×10^{-3} mm^2/s as the strongest indicator of malignancy (20).

These results were compared with Hetta and he showed that the best ADC cutoff value to differentiate between benign and malignant lesions was 1.2×10^{-3} mm^2/s (11).

Palle and Reddy found that the ADC value obtained with low b-values (0 and 150 s/mm^2) is higher than that obtained with higher b-values (499 and 1500 s/mm^2) for all lesion types due to contribution of main perfusion effects to the ADC. So, they calculated the ADC with high b-values (800) to avoid the signal attenuation caused by perfusion effects at low b-values (34).

This study, reported that DWI has higher sensitivity and specificity than those of DCE-MRI in the characterization of breast lesion enhancement. The sensitivity and specificity of breast MR diffusion were 94.4% and 92.1% respectively.

Our results were lower than Abdulghaffar and Tag-Aldeen as they showed that sensitivity and specificity of breast MR diffusion were 95.4% and 97.5%, respectively (35).

Also our results were higher than Kul et al. and they provided 91.5% sensitivity and 86.5% specificity for breast MRI diffusion (10).

In this study the combined DCE-MRI and DWI protocols, provided 97.2% sensitivity and 94.7% specificity in the diagnosis of breast cancer.

These results are higher than the results obtained by Kul et al. who provided 95.7% sensitivity and 89.2% specificity for combined DCE-MRI and DWI protocols (10).

So our study proved that the addition of DWI to DCE-MRI improved the sensitivity and specificity of dynamic contrast enhanced breast MRI by 5.5% and 10.5% respectively.

5. Conflict of Interest

There is no conflict of interest to declare.

References

(1) Catalano O, Nunziata A, Siani A. The breast, in fundamentals in oncologic ultrasound. Sonographic imaging and intervention. Italia: Springer-Verlag; 2009, p. 145–17.
(2) Jansen SA, Fan X, Karczmar S, et al. Differentiation between benign and malignant breast lesions detected by bilateral dynamic contrast-enhanced MRI: a sensitivity and specificity study. Magn Reson Med 2008;59(4):747–54.
(3) Bartholow T, Becich M, Chandran U, Parwani A. Immunohistochemical analysis of ezrin–radixin–moesin-binding phosphoprotein 50 in prostatic adenocarcinoma. BMC Urol 2011;11(1):12.
(4) Huang W, Fisher PR, Dulaimy K, Tudorica LA, O'Hea B. Detection of breast malignancy: diagnostic MR protocol for improved specificity. Radiology 2004;232:585–91.
(5) Warren RML, Pointon L, Thompson D, et al. Reading protocol for dynamic contrast-enhanced MR images of the breast: sensitivity and specificity analysis. Radiology 2005;236:779–88.
(6) Partridge SC, Rahbar H, Murthy R, et al. Improved diagnostic accuracy of breast MRI through combined apparent diffusion coefficients and dynamic contrast enhanced kinetics. Magn Reson Med 2011;65(6):1759–67.
(7) Peters NH, Borel Rinkes IH, Zuithoff NP, Mali WP, Moons KG, Peeters PH. Meta-analysis of MR imaging in the diagnosis of breast lesions. Radiology 2008;246:116–24.
(8) Nunes LW, Schnall MD, Siegelman ES, et al. Diagnostic performance characteristics of architectural features revealed by high spatial resolution MR imaging of the breast. AJR 1997;169:409–15.
(9) Kuhl K, Mielcarek P, Klaschik S, et al. Dynamic breast MR imaging: are signal intensity time course data useful for differential diagnosis of enhancing lesions? Radiology 1999;211:101–10.
(10) Kul S, Cansu A, Alhan E, et al. Contribution of diffusion weighted imaging to dynamic contrast–enhanced MRI in the characterization of breast tumors. Am Roentgen Ray Soc 2011;196:210–7.
(11) Hetta W. Role of diffusion weighted images combined with breast MRI in improving the detection and differentiation of breast lesions. Egyptian J Radiol Nucl Med 2015;46:259–70.
(12) Guo Y, Cai YQ, Cai ZL, et al. Differentiation of clinically benign and malignant breast lesions using diffusion-weighted imaging. J. Magn. Reson. Imaging 2002;16:172–8.
(13) Rubesova E, Grell AS, De Maertelaer V, Metens T, Chao SL, Lemort M. Quantitative diffusion imaging in breast cancer: a clinical prospective study. J Magn Reson Imaging 2006;24:319–24.
(14) Woodhams R, Matsunaga K, Kan S, et al. ADC mapping of benign and malignant breast tumors. Magn Reson Med Sci 2005;4:35–42.
(15) Hatakenaka M, Soeda H, Yabuuchi H, et al. Apparent diffusion coefficients of breast tumors: clinical application. Magn Reson Med Sci 2008;7:23–9.

(16) Marini C, Iacconi C, Giannelli M, Cilotti A, Moretti M, Bartolozzi C. Quantitative diffusion weighted MR imaging in the differential diagnosis of breast lesion. Eur Radiol 2007;17:2646–55.

(17) Lo GG, Ai V, Chan JK, et al. Diffusion-weighted magnetic resonance imaging of breast lesions: first experiences at 3 T. J Comput Assist Tomogr 2009;33:63–9.

(18) Tozaki M, Fukuma E. 1H MR spectroscopy and diffusion-weighted imaging of the breast: are they useful tools for characterizing breast lesions before biopsy? AJR 2009;193:840–9.

(19) Partridge SC, DeMartini WB, Kurland BF, Eby PR, White SW, Lehman CD. Differential diagnosis of mammographically and clinically occult breast lesions on diffusion-weighted MRI. J Magn Reson Imaging 2010;31:562–70.

(20) Yabuuchi H, Matsuo Y, Okafuji T, et al. Enhanced mass on contrast-enhanced breast MR imaging: lesion characterization using combination of dynamic contrast-enhanced and diffusion-weighted MR images. J Magn Reson Imaging 2008;28:1157–65.

(21) Partridge SC, DeMartini WB, Kurland BF, Eby PR, White SW, Lehman CD. Quantitative diffusion-weighted imaging as an adjunct to conventional breast MRI for improved positive predictive value. AJR 2009;193:1716–22.

(22) Kriege M, Brekelmans CT, Boetes C, et al. Efficacy of MRI and mammography for breast cancer screening in women with a familial or genetic predisposition. N Engl J Med 2004;351:427–37.

(23) Warner E, Plewes D B, Hill K A, et al. Surveillance of BRCA1 and BRCA2 mutation carriers with magnetic resonance imaging, ultrasound, mammography, and clinical breast examination. J Am Med Assoc 2004;292(11):1317–25.

(24) Leach MO, Boggis CR, Dixon AK, et al. Screening with magnetic resonance imaging and mammography of a UK population at high familial risk of breast cancer: a prospective multicentre cohort study (MARIBS). Lancet 2005;365(9473):1769–78.

(25) Mahoney CM. Breast imaging: mammography, sonography and emerging technology. In: Donegan LW, Spratt SJ, editors. Cancer of the breast. Philadelphia: Elsevier Science; 2002.

(26) Darbre DPH. Recorded quadrant incidence of female breast cancer in Great Britain suggests a disproportionate increase in the upper outer quadrant of the breast. Anti Cancer Res 2005;25:2543–50.

(27) Li CI, Uribe DJ, Daling JR. Clinical characteristics of different histological types of breast cancer. Br J Cancer 2005;93(9):1046–52.

(28) Wedegärtner U, Bick U, Wörtler K, Rummeny E, Bongartz G. Differentiation between benign and malignant findings on MR-mammography: usefulness of morphological criteria. Eur Radiol 2001;11(9):1645–50.

(29) Tozaki M, Igarashi T, Fukuda K. Positive and negative predictive values of BI-RADS descriptors for focal breast masses. Magn Reson Med Sci 2006;5(1):7–15.

(30) Mahoney MC, Gatsonis C, Hanna L, et al. Positive predictive value of BI-RADS MR imaging. Radiology 2012;264(1):51–8.

(31) Morris EA, Liberman L. Breast atlas. In: Breast MRI, editor. Diagnosis and intervention. New York: Springer Science; 2005. p. 329–448.

(32) Kuhl CK, Schild HH, Morakkabati N. Dynamic bilateral contrast-enhanced MR imaging of the breast: trade-off between spatial and temporal resolution. Radiology 2005;236:789–800.

(33) Malich A, Fischer RD, Wurdinger S, et al. Potential MRI interpretation model: differentiation of benign from malignant breast masses. AJR 2005;185:964–70.

(34) Palle L, Reddy B. Role of diffusion MRI in characterizing benign and malignant breast lesions. Indian J Radiol Imaging 2009;19(4):287–90.

(35) Abdulghaffar W, Tag-Aldeen M. Role of diffusion-weighted imaging (DWI) and apparent diffusion coefficient (ADC) in differentiating between benign and malignant breast lesions. Egyptian J Radiol Nucl Med 2013;44:945–51.